FEBS Open Bio 2 (2012) 313–317

journal homepage: www.elsevier.com/locate/febsopenbio

Co-mutation of histone H2AX S139A with Y142A rescues Y142A-induced ionising radiation sensitivity

James A.L. Brown[1,*], John K. Eykelenboom, Noel F. Lowndes[*]

Genome Stability Laboratory, Centre for Chromosome Biology, School of Natural Sciences, National University of Ireland, Galway, Galway, Ireland

ARTICLE INFO

Article history:
Received 18 September 2012
Accepted 26 September 2012

Keywords:
H2AX
Y142
S139
DSB
IR
53BP1

ABSTRACT

Under normal conditions histone H2AX is constitutively phosphorylated on tyrosine (Y) 142 by Williams–Beuren syndrome transcription factor kinase (WSTF). Following DNA double strand breaks (DSB), Y142 is de-phosphorylated and serine (S) 139 is phosphorylated. Here we explored DSB-dependent cross talk between H2AX residues S139 and Y142. *H2axY142A* mutation resulted in increased sensitivity to ionising radiation (IR), compared to *H2axS139A*. Interestingly, co-mutation of S139A and Y142A rescued IR sensitivity. The DSB response proteins 53Bp1 and Rad51 were recruited to IR-induced foci (IRIF) in *H2axS139A*, *H2axY142A* and *H2axS139A/Y142A* cells. Our results suggest that *H2axY142A* IR sensitivity is dependent upon the C-terminal residue, S139.

1. Introduction

One of the earliest cellular events upon induction of DNA double strand breaks (DSB) is ATM-dependent phosphorylation of histone H2AX on Serine (S) 139 [1]. Although this modification, termed γH2AX, is the most characterised post-translational modification of H2AX, other DSB-induced modifications of H2AX have been described on lysines 5 and 36 and threonine 101 [2–4]. In higher eukaryotes the Williams–Beuren syndrome transcription factor kinase (WSTF) constitutively phosphorylates H2AX at it C-terminal residue, tyrosine 142, termed H2AXY142ph [5]. The H2AXY142ph modification is abrogated following DSB by the counteracting activity of the EYA phosphatases [5–7]. Perturbing either of these events impacts on DNA damage response signalling, through ATM, leading to increased cell death following DNA damage [5,6]. It has been proposed that persistence of Y142 phosphorylation on H2AX following DNA damage leads to apoptosis while de-phosphorylation facilitates repair [8]. Recently, a qualitative correlation between H2AX Y142 de-phosphorylation and γH2AX formation has been described, suggesting cross talk between these two modified residues [5].

Here we use the DT40 model system, a chicken B lymphocytic cell line that facilitates gene targeting, to introduce mutations into chicken *H2ax* that result in single and double substitutions of residues S139 and Y142 to alanines (A). This model system recapitulates many key features seen in higher vertebrate systems and *Gallus gallus* H2ax has high sequence homology to human H2AX [9,10]. As the mutant H2ax proteins are the sole source of H2ax in these cells we then explored the relationship between these two C-terminal DNA damage responsive sites of phosphorylation. We found that although expression of H2ax-Y142A resulted in slow growth and radio-sensitivity, co-mutation of residue S139A on the same molecule rescued the Y142A associated phenotypes. Repression of the H2ax-Y142A phenotype, by co-mutation of S139A, is likely due to loss of signalling associated with non-modifiable S139A residue.

2. Material and methods

2.1. Cell culture conditions

The DT40 chicken B lymphocyte cell lines were cultured as previously described [10]. Briefly, DT40 cell lines were cultured at 39.5 °C and 5.0% CO_2 in RPMI 1640 and 10% foetal bovine serum (FBS) [Lonza (Berkshire, UK)], 1% chicken serum, 100 U/ml penicillin and 100 μg/ml streptomycin [Sigma (Dublin, Ireland)].

Abbreviations: DSB, DNA double strand break; IR, ionising radiation; WSTF, Williams–Beuren syndrome transcription factor kinase; IRIF, ionising radiation induced foci; WT, Wild type; F, phenylalanine; W, tryptophan; A, alanine; Y, tyrosine; Fig, Figure; RT-PCR, reverse transcription polymerase chain reaction; H2AX/H2ax, MDC1/Mdc1, RAD51/Rad51 and 53BP1/53Bp1, indicate human or mouse/chicken proteins respectively

[1] Current address: Systems Biology Ireland, Regenerative Medicine Institute, National Centre of Biomedical Engineering, National University of Ireland, Galway, Galway, Ireland.

[*] Corresponding authors.

E-mail addresses: james.brown@nuigalway.ie (J.A.L. Brown) noel.lowndes@nuigalway.ie (N.F. Lowndes).

2211-5463/$36.00
http://dx.doi.org/10.1016/j.fob.2012.09.008

2.2. H2AX targeting vectors and PCR primers used

The DT40 *H2ax* mutants were created using site directed mutagenesis of the *Gallus gallus H2ax* gene, subcloned from the previously described vector [12]. Amplification primers for the *Gallus gallus H2ax* open reading frame used were; forward 5′-CGCGGCAAGAGTGGCGGTAA-3′ and reverse 5′-AGCATGGGCTATTGCAGGACCC-3′.

Mutations were introduced using site directed mutagenesis (Stratagene) as per manufacturers instructions. Mutation specific primer sequences were: S139A 5′-CAGCGGGCAGCAGGCCCAGGAGTACTAGG-3′, Y142A 5′-CAGTCGCAGGAGGCCTAGCCCACCC-3′ and S139A/Y142A 5′-GCGGGCAGCAGGCCCAGGAGGCCTAGGCCTGGC-3′. All mutations introduced were verified by DNA sequencing.

The ovalbumin targeting vector was constructed as follows: ovalbumin homology arms were amplified from DT40 genomic DNA by PCR with KOD polymerase (Novagen) using the following primer pairs: 5′ ovalbumin arm: 5′-AAAAAGCGGCCGCCAGGAAGCTTTAAGGAATCATTG-3′ and 5′-CCCAGAACTAGTGGATCCTGGATGGGAGAGAAGACTGG-3′. 3′ ovalbumin arm: 5′- CATCCAGGATCCACTAGTTCTGGGACAGTTTGCTACCC-3′ and 5′- AAAAAGTCGACCTCAGTGCACAGGAATGGAG-3′. Homology arms were cloned into ploxPuro1 with a puromycin resistance cassette under the control of the CMV promoter inserted between the arms. The H2ax mutants were inserted using Nhe1 sites and all constructs verified by sequencing. All constructs were linearised by Pvu1 digestion and transfection performed as previously described [11]. Southern blot screening was carried out using a probe external to the targeting construct. The probe was amplified and labelled with α-32P using the forward primer 5′-TTTATGGGGGAAAAATGCAG-3′ and the reverse primer 5′-CAGATGAGTTGTCCCAGGTG-3′.

2.3. Proliferation and clonogenic survival analysis

For cell growth analysis, cultures were seeded in triplicate at equal cell densities (1×10^4 cells/ml) and counted using a haemocytometer every 24 h. Survival following ionising radiation treatment [137Cs irradiator (Mainance Engineering Ltd., UK), dose rate of 21.57 Gy/min] was determined by clonogenic survival assays in methylcellulose medium. Colonies formed by surviving cells were counted 7–10 days later. Results normalised to number of cells plated.

2.4. Antibodies

Western blotting was performed using the antibody recognising phosphorylated H2AX Y142 (Millipore). Immunofluorescent antibodies; 53Bp1 (Millipore) and Rad51 (ab63801, Abcam) and FITC or Texas Red-conjugated secondary antibodies (Jackson Immunoresearch).

2.5. Immunofluorescence microscopy and foci quantification

Cells were bound to poly-L-lysine coated slides prior to fixation in 4% paraformaldehyde and permeabilisation in 0.1% Triton-X-100. Cells were then blocked in 1% BSA and incubated with the indicated antibodies overnight at 4 °C.

Images acquired with an Olympus IX71 inverted microscope equipped with a Retiga-EXL Mono Lightwire 800 camera (QImaging, British Colmbia, Canada) and Image Pro-Plus software (Media Cybernetics Inc., Bethesda, USA). 0.4 μm Z-stacks were collected and brightest point projections created from stacked sections. All cell percentages were obtained from blind counting of 80–100 cells per sample. All foci percentages were determined using Cell Profiler software [13] counts of 50–100 cells per sample. Only cells with intact nuclei, no blebbing as determined by DAPI staining, were included in the counts.

2.6. Fluorescence activated flow cytometry

Cells were fixed in 70% ethanol at 4 °C overnight. Cells were then stained using propidium iodide (Sigma, Dublin, Ireland), and analysed using the FACS Calibur platform and CellQuest software (BD Biosciences, Belgium).

3. Results

3.1. H2ax mutation approach and cell line construction

To examine the role of *Gallus gallus* H2ax residues S139 and Y142 in the DSB response we generated cell lines containing S139A, Y142A and S139A/Y142A mutations. Mutation of Y142 to phenylalanine or tryptophan, which would maintain the aromatic character of this residue, was not performed as such conservative substitutions may imitate IR induced de-phosphorylation events. This possibility is supported by the lack of disruption of either 53BP1 or MDC1 ionising radiation induced foci (IRIF) when these conservative mutations were employed [2,3]. Furthermore, the *H2ax-Y142A* mutation has been shown to perturb Mdc1 recruitment to IRIF in mouse cells [14]. Using a previously generated *Gallus gallus* DT40 *H2ax*$^{-/-}$ (null) cell line [12]. Constructs harbouring S139A, Y142A or S139A/Y142A *H2ax* mutations were targeted to the ovalbumin (*Ova*) locus. This generated three cell lines, termed *H2ax-S139A*, *H2ax-Y142A* and *H2ax-S139A/Y142A*, which express the indicated *H2ax* mutant allele as the sole source of H2ax protein in these cells. As the introduced mutations disrupt the binding of anti-H2AX antibodies from multiple sources, as previously was previously described [2], expression of each mutant was therefore confirmed by RT-PCR (Fig. 1(A)). Isogenic cells expressing wild-type *H2ax* (WT) were used as a control for all experiments.

It has previously been reported in human cells that phosphorylation of H2AX at its terminal Y142 residue is abrogated following DSB [5]. Following ionising radiation (IR) treatment we confirmed that de-phosphorylation of H2AX Y142 occurred in our WT DT40 cells, thereby validating our system (Fig. 1(B)). The direct effect of the H2AX mutations on the phosphorylation of Y142 could not be confirmed by western blotting, due to the disruption of H2AX antibody binding referred to above. Therefore, we examined the effect of the H2ax mutations on other cellular process.

3.2. H2ax-Y142A mutation results in slow growth and IR sensitivity

Relative to WT we found *H2ax-Y142A* cells exhibited a slow growth phenotype that was more pronounced than either *H2ax-S139A* or null cells (Fig. 2(A)). Significantly, in *H2ax-S139A/Y142A* cells, in which all H2ax molecules harbour both substitutions, the slow growth phenotype of *H2ax-Y142A* is rescued, with growth restored to levels seen in *H2ax-S139A* cells.

To further explore the relationship between these residues, their effect on cellular survival after ionising radiation was examined. In response to low-dose IR it was previously reported that *H2ax-Y142A* cells exhibited a mild sensitivity in mouse ES cells [2]. We found that our *H2ax-Y142A* DT40 cells displayed a higher sensitivity to IR, particularly at high dose (8 Gy) treatments not examined in previous studies [2] (Fig. 2(B)). Consistent with previous reports [12], our Null cells displayed sensitivity to IR relative to WT. Significantly, the double mutant, *H2ax-S139A/Y142A*, showed WT levels of IR sensitivity.

3.3. H2ax-Y142A mutations lead to increased constitutive cell death

To investigate a possible mechanism for the *H2ax-Y142A* mediated phenotype we performed cell cycle analyses. *H2ax-Y142A* cells displayed an increased apoptotic sub-G1 fraction prior to damage (Fig. 2(C)). Again, in *H2ax-S139A/Y142A* cells this phenotype was suppressed. Following IR treatment the same trend of apoptosis was

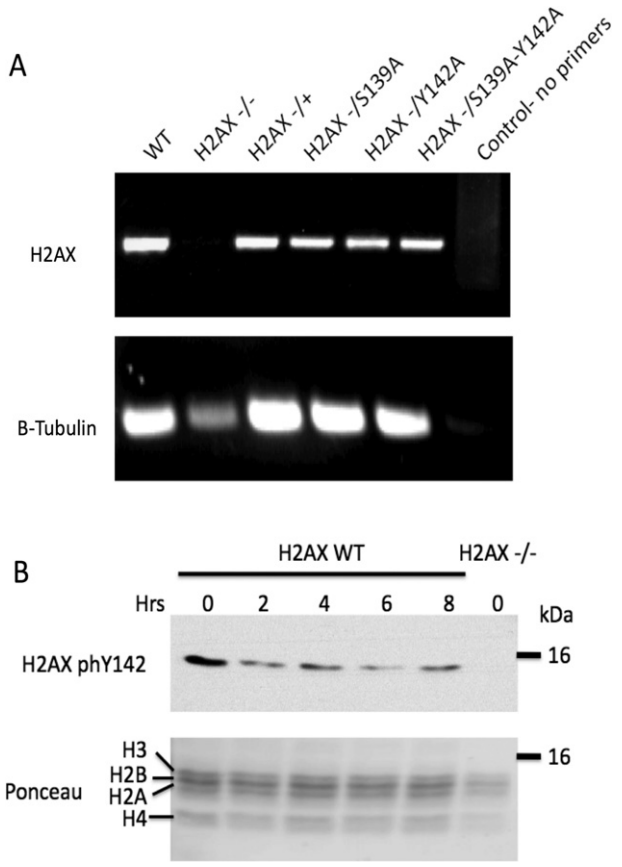

Fig. 1. (A) Amplification of *H2ax* from mRNA isolated from indicated cell lines, $N = 3$. (B) Kinetics of H2ax phosphorylation on residue Y142 following 10 Gy IR.

observed in all cell lines, with *H2ax-S139A/Y142A* cells displaying virtually WT levels of Sub-G1 cells. However, following IR there was a significant reduction in the number of cells observed in G2/M in *H2ax-Y142A* cells (Fig. 2(D)). Again this was restored to almost WT levels in *H2ax-S139A/Y142A* cells.

3.4. H2ax-Y142A and H2ax-S139A/Y142A cells can form 53Bp1 IRIF

The constitutively high levels of sub-G1 cells observed in H2ax-Y142A cells suggested they might have intrinsic DNA damage. As previously reported [2], C-terminal mutations of tyrosine 142 of human H2AX interfere with detection of γH2AX IRIF and similarly we were unable to observe γH2ax foci in cells harbouring our *H2ax* mutations. Therefore, to explore the DNA damage response we examined recruitment of the DNA repair proteins 53Bp1 and Rad51 to IRIF (Fig. 3(A)). We used 53Bp1 foci formation as a surrogate for γH2AX, as 53Bp1 forms IRIF with kinetics very similar to γH2AX IRIF [16].

All cell lines were able to form 53Bp1 IRIF that persisted for at least 8 h post IR treatment (Fig. 3(A)). Quantification of the number of cells displaying 53Bp1 foci revealed that while *H2ax-S139A* cells have elevated levels of endogenous 53Bp1 foci, *H2ax-S139A/Y142A* cells have reduced levels of endogenous foci compared to the control (WT, Null) and *H2ax-S139A* cells (Fig. 3(B), right panel). Following IR treatment similar numbers of cells positive for 53Bp1 IRIF were observed (Fig. 3(B), far right).

Prior to treatment few cells in any line displayed Rad51, a DSB repair protein, foci (Fig. 3(C), far left panel). However, following IR treatment we found a significant increase in *H2ax-S139A* cells displaying Rad51 IRIF compared to WT and null cells. Furthermore, although there was an overall increase in Rad51 positive cells in all lines, when comparing between the *H2ax* mutants the increase in

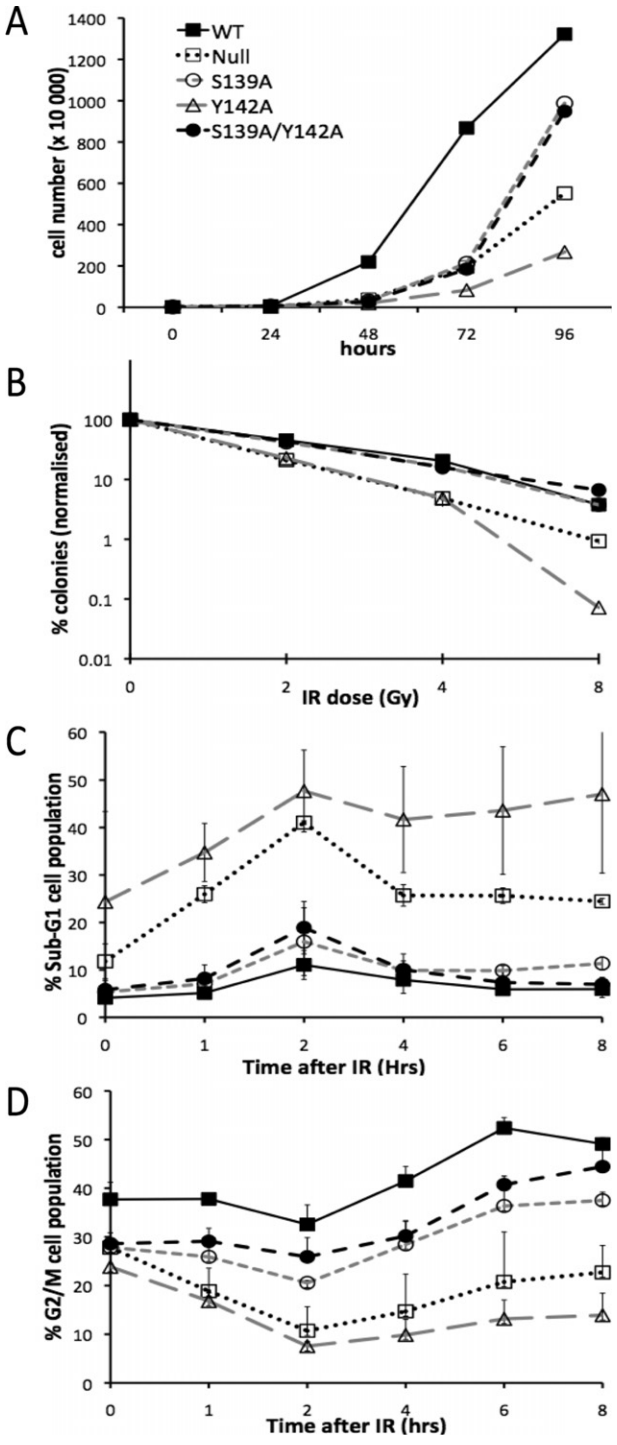

Fig. 2. (A) Growth kinetics of indicated *H2ax* mutant expressing cells, $N = 3$. (B) Clonogenic IR survival of indicated *H2ax* mutant cell lines following indicated IR dose, $N = 3$. (C) Percent of cells in Sub G1 fraction following IR (10 Gy) treatment, $N = 3$. (D) Percent of cells in G2 fraction following IR (10 Gy) treatment, $N = 3$. Legend in (A) applies to all.

H2ax-Y142A and *H2ax-S139A/Y142A* cells was significantly smaller, ($p = 0.011$) and ($p = 0.037$) respectively, than the increase observed in *H2ax-S139A* cells (Fig. 3(B), centre).

Further investigation of 53Bp1 IRIF, by quantifying the number of 53Bp1 IRIF per cell revealed that null, *H2ax-S139A* and *H2ax-S139A/Y142A* cells had increased numbers of 53Bp1 IRIF per cell compared to WT (Fig. 3(C)). Significantly, the null and *H2ax-S139A/Y142A* cells have approximately the same increase in IRIF, while *H2ax-S139A* have

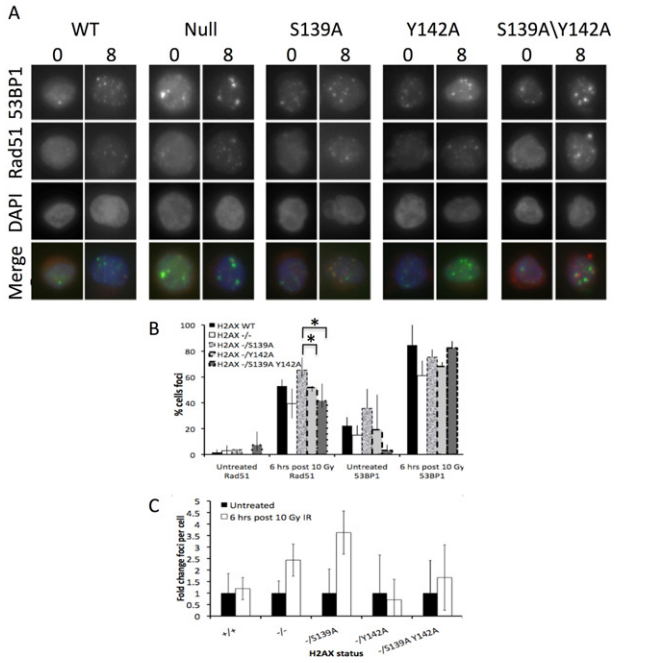

Fig. 3. A: Localisation of 53Bp1 and Rad51 in indicated H2ax mutants following IR (8 Gy) treatment at indicated time points, $N = 2$. (B) Percent of cells with either 53Bp1 (>3) or Rad51 (>1) foci following IR (8 Gy) treatment, $N = 2$. Greater than 50 cells counted per time point per experiment. * ≥0.05 significance, students *T*-test. (C) Fold change in numbers of 53Bp1 IRIF per cell in indicated H2ax mutants following IR (8 Gy) treatment.

more 53Bp1 IRIF per cell than these two lines. Although it is difficult to accurately assess 53Bp1 IRIF in *H2ax-Y142A* cells, due to the high level of cell death, the surviving fraction assayed displayed WT levels of 53Bp1 IRIF.

4. Discussion

In this study we demonstrate that cells expressing H2ax-Y142A, as the sole source of histone H2AX, display increased constitutive cell death and IR sensitivity. Interestingly, we found that combining the S139A and Y142A substitutions on the same H2AX molecule resulted in a suppression of the H2ax-Y142A mediated phenotypes. Furthermore, our results support the finding that DNA repair can occur, at a reduced rate, in the absence of phosphorylation at H2AX S139 [12,18].

Our analysis of cell proliferation indicates that *H2ax-Y142A* cells are slow growing due to an higher rate of constitutive cell death, indicated by an increased sub-G1 population (Fig. 2(A) and (C)). We propose that this is due to endogenous DNA damage which is supported by *H2ax-Y142A* cells displaying increased levels of constitutive 53Bp1 foci, indicative of DNA damage. As the double mutant, *H2ax-S139A/Y142A,* rescues this sensitivity (Figs. 2(C) and 3(C)) this suggests that the Y142A sensitivity to IR induced cell death (Fig. 2(B)) relies on signalling involving the S139 residue. *H2ax-Y142A* cells appear able to initiate DSB repair, as 53Bp1 is still recruited to sites of damaged DNA. However, the overall reduction in Rad51 IRIF (Fig. 3(B)) and 53Bp1 IRIF observed in *H2ax-Y142A* cells following DNA damage (Fig. 3(C)) is likely an under-estimation, influenced by the increased rates of cell death (see Fig. 2(C)) removing damaged cells. The observed radio-sensitivity of *H2ax-Y142A* cells is likely due to impairment of the homologous recombination (HR) DNA repair pathway (which has been previously reported in mouse H2ax-Y142A expressing mutant cells [2,3]) as HR is the major DNA damage repair pathway utilised by DT40 cells. In addition, it was previously demonstrated that the conservative H2AX mutations, Y142F or Y142W both of which would mimic de-phosphorylation, do not significantly affect the HR pathway [2,3]. This underscores the importance of active de-phosphorylation at H2AX Y142 for correct DNA repair and maintenance.

H2ax-S139A/Y142A DT40 cells display 53Bp1 IRIF suggesting that localisation of 53Bp1 at DSBs is at least partially independent of modifications to either the Y142 or S139 H2AX residues. Human 53BP1 binding is known to be mediated, at least in part, through MDC1 and as MDC1 cannot bind to H2AX without phosphorylated S139 and de-phosphorylated Y142 [15], this indicates that 53BP1 IRIF formation must not be solely dependent on H2AX mediated MDC1 localisation. Our results are consistent with previously described mouse H2AX$^{-/-}$ cells, which can form 53BP1 IRIF, although the number of 53BP1 foci is significantly reduced in this mouse system [14]. How the S139A and Y142A mutants effect Mdc1 binding in our system is unknown, as no working antibody exists for *Gallus gallus* Mdc1. However, an explanation for the observed recruitment of 53BP1 to DSB is that this localisation is mediated through the previously described interaction of MDC1 with the MRN complex [17,14].

H2ax-S139A/Y142A cells display less Rad51 IRIF compared to *H2ax-S139A*, suggesting that *H2ax-S139A/Y142A* cells can repair the damaged DNA more efficiently. Recent results support our finding that cells can actively repair DNA in the absence of γH2AX and other sites on H2AX have been suggested to play a role [18]. Our *H2ax-Y142A* cells also display fewer cells positive for Rad51 IRIF, which could be explained by more cells undergoing apoptosis (Fig. 3(B)).

Taken together our results indicate the H2AX mediated response to DSB is more complicated than expected. Although modification of H2AX S139 is important for the DSB response, modifications of the H2AX Y142 residue, either phosphorylation or de-phosphorylation, clearly play a significant role in determining cell fate in conjunction with phosphorylation at H2AX S139.

Statement of contribution

JALB: conception and design of the work, acquisition of all data, analysis and interpretation of data, wrote the manuscript. JKE: provided reagents. NFL: project conception, analysis and interpretation of data, edited the manuscript.

Acknowledgments

The authors wish to thank the Lowndes' group and the CCB for stimulating discussions; Dr. Muriel Grenon and Dr. Emer Bourke for critical comments on the manuscript. We also would like to thank Prof. Takeda for his kind gift of the *H2ax*$^{-/-}$ DT40 cells and the Wild Type *H2ax* vector.

References

[1] Rogakou E.P., Pilch D.R., Orr A.H., Ivanova V.S., Bonner W.M. (1998) DNA double-stranded breaks induce histone H2AX phosphorylation on serine 139. J. Biol. Chem. 273(10), 5858–5868.
[2] Xie A., Odate S., Chandramouly G., Scully R. (2010) H2AX post-translational modifications in the ionizing radiation response and homologous recombination. Cell Cycle. 9(17), 3602–3610.
[3] Xie A., Hartlerode A., Stucki M., Odate S., Puget N., Kwok A. et al. (2007) Distinct roles of chromatin-associated proteins MDC1 and 53BP1 in mammalian double-strand break repair. Mol. Cell. 28(6), 1045–1057.
[4] Jiang X., Xu Y., Price B.D. (2010) Acetylation of H2AX on lysine 36 plays a key role in the DNA double-strand break repair pathway. FEBS Lett. 584(13), 2926–2930.
[5] Xiao A., Li H., Shechter D., Ahn S.H., Fabrizio L.A., Erdjument-Bromage H. et al. (2009) WSTF regulates the H2A.X DNA damage response via a novel tyrosine kinase activity. Nature. 457(7225), 57–62.
[6] Cook P.J., Ju B.G., Telese F., Wang X., Glass C.K., Rosenfeld M.G. (2009) Tyrosine dephosphorylation of H2AX modulates apoptosis and survival decisions. Nature. 458(7238), 591–596.
[7] Krishnan N., Jeong D.G., Jung S.K., Ryu S.E., Xiao A., Allis C.D. et al. (2009) Dephosphorylation of the C-terminal tyrosyl residue of the DNA damage-related histone H2A.X is mediated by the protein phosphatase eyes absent. J. Biol. Chem. 284(24), 16066–16070.

[8] Banerjee T., Chakravarti D. (2011) A peek into the complex realm of histone phosphorylation. Mol. Cell Biol. 31(24), 4858–4873.
[9] Li A., Yu Y., Lee S.C., Ishibashi T., Lees-Miller S.P., Ausió J. (2010) Phosphorylation of histone H2A.X by DNA-dependent protein kinase is not affected by core histone acetylation, but it alters nucleosome stability and histone H1 binding. J. Biol. Chem. 285(23), 17778–17788.
[10] Caldwell R.B., Fiedler P., Schoetz U., Buerstedde J.M. (2007) Gene function analysis using the chicken B-cell line DT40. Methods Mol. Biol. 408, 193–210.
[11] FitzGerald J., Moureau S., Drogaris P., O'Connell E., Abshiru N., Verreault A. et al. (2011) Regulation of the DNA damage response and gene expression by the Dot1L histone methyltransferase and the 53Bp1 tumour suppressor. PLoS ONE. 6(2), e14714.
[12] Sonoda E., Zhao G.Y., Kohzaki M., Dhar P.K., Kikuchi K., Redon C. et al. (2007) Collaborative roles of gammaH2AX and the Rad51 paralog Xrcc3 in homologous recombinational repair. DNA Repair (Amst). 6(3), 280–292.
[13] Kamentsky L., Jones T.R., Fraser A., Bray M., Logan D., Madden K. et al. (2011) Improved structure, function, and compatibility for CellProfiler: modular high-throughput image analysis software. Bioinformatics. 27(8), 1179–1180.
[14] Stucki M., Clapperton J.A., Mohammad D., Yaffe M.B., Smerdon S.J., Jackson S.P. (2005) MDC1 directly binds phosphorylated histone H2AX to regulate cellular responses to DNA double-strand breaks. Cell. 123(7), 1213–1226.
[15] Lee M.S., Edwards R.A., Thede G.L., Glover J.N. (2005) Structure of the BRCT repeat domain of MDC1 and its specificity for the free COOH-terminal end of the {gamma}-H2AX histone tail. J. Biol. Chem. 280, 32053–32056.
[16] Xu X., Stern D.F. (2003) NFBD1/MDC1 regulates ionizing radiation-induced focus formation by DNA checkpoint signaling and repair factors. FASEB J. 17, 1842–1848.
[17] Schultz L.B., Chehab N.H., Malikzay A., Halazonetis T.D. (2000) p53 binding protein 1 (53BP1) is an early participant in the cellular response to DNA double-strand breaks. J. Cell Biol. 151(7), 1381–1390.
[18] Revet I., Feeney L., Bruguera S., Wilson W., Dong T.K., Oh D.H. et al. (2011) Functional relevance of the histone gammaH2Ax in the response to DNA damaging agents. Proc. Natl. Acad. Sci. USA. 108(21), 8663–8667.